21. R. G. Parr, W. Yang, *Density Functional Theory of Atoms and Molecules* (Oxford Univ. Press, New York, 1989).
22. M. Khalil, N. Demirdoven, A. Tokmakoff, *J. Chem. Phys.* **121**, 362 (2004).
23. H.-S. Tan, I. R. Piletic, M. D. Fayer, *J. Opt. Soc. Am. B* **22**, 2009 (2005).
24. V. Pophristic, L. Goodman, *Nature* **411**, 565 (2001).
25. F. M. Bickelhaupt, E. J. Baerends, *Angew. Chem. Int. Ed.* **42**, 4183 (2003).
26. We thank X. Chen and J. I. Brauman for insightful discussions. This work was supported by grants from the Air Force Office of Scientific Research (F49620-01-1-0018) and NSF's Division of Materials Research (DMR-0332692).

Supporting Online Material
www.sciencemag.org/cgi/content/full/313/5795/1951/DC1
Figs. S1 to S3
References

6 July 2006; accepted 21 August 2006
10.1126/science.1132178

Soluble Mn(III) in Suboxic Zones

Robert E. Trouwborst,[1] Brian G. Clement,[2] Bradley M. Tebo,[3] Brian T. Glazer,[1]* George W. Luther III[1]†

Soluble manganese(III) [Mn(III)] has been thought to disproportionate to soluble Mn(II) and particulate $Mn^{IV}O_2$ in natural waters, although it persists as complexes in laboratory solutions. We report that, in the Black Sea, soluble Mn(III) concentrations were as high as 5 micromolar and constituted up to 100% of the total dissolved Mn pool. Depth profiles indicated that soluble Mn(III) was produced at the top of the suboxic zone by Mn(II) oxidation and at the bottom of the suboxic zone by $Mn^{IV}O_2$ reduction, then stabilized in each case by unknown natural ligands. We also found micromolar concentrations of dissolved Mn(III) in the Chesapeake Bay. Dissolved Mn(III) can maintain the existence of suboxic zones because it can act as either an electron acceptor or donor. Our data indicate that Mn(III) should be ubiquitous at all water column and sediment oxic/anoxic interfaces in the environment.

Manganese is essential in a variety of biogeochemical processes from photosynthesis to bacterially mediated organic matter decomposition (*1*, *2*). It acts as a catalyst in an important microbially mediated redox cycle to oxidize and detoxify H_2S; Mn(II) is first oxidized by O_2 to MnO_2 (*3*, *4*), which then oxidizes H_2S with re-formation of Mn(II) (*5*–*8*). Traditionally, dissolved manganese (material passing through 0.2- or 0.4-μm filters) has been assumed to be Mn(II), whereas particulate manganese has been assumed to exist only as MnO_2 because any inorganic Mn(III) formed would disproportionate to Mn(II) and Mn(IV). However, soluble Mn(III) can be stabilized with organic chelates and inorganic chelates (e.g., pyrophosphate, a particularly good chelating agent) to prevent disproportionation and is well known in laboratory solutions (*9*–*14*). Because its existence as a major chemical species has not been documented in the aquatic environment, soluble Mn(III) has become an overlooked Mn species.

Because the d_{z^2} and $d_{x^2-y^2}$ orbitals that can accept electrons in MnO_2 or donate electrons from Mn(II) are spatially distinct, reduction of MnO_2 or oxidation of Mn(II) should lead to Mn(III) species via one-electron transfer processes (*15*). Possible natural sources of soluble Mn(III) include photosynthetic reaction centers released during phytoplankton decomposition, as well as its formation as an intermediate in the bacterial oxidation of Mn(II) → Mn(IV) (*16*) and reduction of Mn oxides with sulfide (*17*). The Mn(III) formed can then be complexed by a variety of ligands that include pyrophosphate (formed from the breakdown of adenosine 5′-triphosphate or adenosine 5′-diphosphate), siderophores that bind extracellular Fe(III) and Mn(III) with similar binding strengths, or other natural ligands (*9*–*14*).

Once formed, Mn(III) is an important one-electron transfer redox species that can act as either an oxidant or a reductant. Mn(III) is an ideal chemical species to maintain the existence of suboxic zones, which have dissolved O_2 and H_2S below normal detection levels. Suboxic zones are ubiquitous as they are found in sedimentary porewaters of lakes, estuaries, bays, and oceans; in permanently anoxic basins (the Black Sea, the Arabian Sea, equatorial Pacific, and fjords); and in shallower seasonally anoxic basins (the Chesapeake Bay and Saanich Inlet).

To test the hypothesis that soluble Mn(III) is present and a key redox species in the Mn catalytic redox cycle, we used known Mn(III) coordination chemistry to search for Mn(III) in the suboxic waters of the Black Sea and the Chesapeake Bay. We used in situ voltammetry (*18*–*20*) to simultaneously measure O_2 and H_2S (defined as the sum of H_2S, HS^-, S_x^{2-}, and S_8) in one cast. Once the suboxic zone was documented, we used traditional bottle methods on a subsequent cast to obtain samples for total dissolved Mn, particulate Mn (*21*), and dissolved Mn(III). Dissolved Mn is defined as that material which passes through 0.2-μm Nuclepore filters. This approach can separate soluble Mn(III) from particulate MnO_x. Previous marine and estuarine studies (*22*, *23*) that used radiotracer Mn showed that all size-fractionated particulate MnO_x is trapped on 1.0-μm or smaller filters as Mg^{2+} and Ca^{2+} induce MnO_2 precipitation (*24*). X-ray absorption near-edge spectroscopy measurements (*25*) have documented that particulate MnO_x from Black Sea waters, formed by microbially mediated Mn(II) oxidation, is in the Mn(IV) state and similar to δ-MnO_2.

To measure Mn(III) in field samples, we used cathodic stripping voltammetry to detect Mn(III) as the known desferrioxamine-B (DEF-B) complex (*9*). Samples were collected in gas-tight syringes directly from a Niskin bottle and then filtered in an argon-filled glove bag. After running background voltammograms to determine that H_2S and O_2 were not measurable in the sample, we added DEF-B as a competitive ligand to 10 ml of sample so that the total concentration was 20 μM. DEF-B gives a ligand peak at –1.34 V versus saturated calomel electrode (SCE), and the Mn(III)DEF-B complex has a signal at –1.19 V versus SCE (Fig. 1). This procedure was calibrated with 1 to 5 μM Mn(III)pyrophosphate standards (fig. S1). DEF-B complexed all dissolved Mn(III) in standards and in samples within 30 s of mixing, indicating that DEF-B complexed Mn(III) more strongly than pyrophosphate, as expected on the basis of the known stability constants of

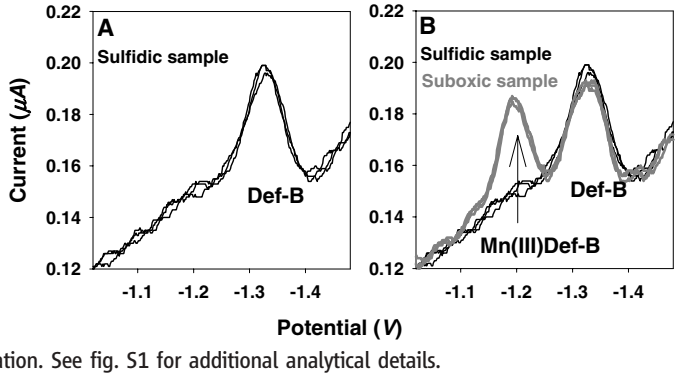

Fig. 1. (**A**) Free desferrioxamine-B (DEF-B) ligand signal at −1.34 V in a sample without Mn(III) complexes (oxic or sulfidic sample). (**B**) Mn(III)DEF-B complex signal at −1.19 V and the free ligand signal at −1.34 V in a sample from the suboxic region of the Black Sea. The free-ligand DEF-B peak decreased due to complexation. See fig. S1 for additional analytical details.

[1]College of Marine and Earth Studies, University of Delaware, Lewes, DE 19958, USA. [2]Marine Biology Research Division, Scripps Institution of Oceanography, University of California, San Diego, 9500 Gilman Drive, La Jolla, CA 92093–0202, USA. [3]OGI School of Science and Engineering, Oregon Health and Science University, 20000 NW Walker Road, Beaverton, OR 97006, USA.

*Present address: Department of Oceanography, University of Hawaii, 1000 Pope Road, Honolulu, HI 96822, USA.
†To whom correspondence should be addressed. E-mail: luther@udel.edu

Mn(III) with pyrophosphate and DEF-B (*10*, *14*) and other natural ligands. The Mn(III)DEF-B and Mn(III)pyrophosphate complexes are stable but are reduced by H_2S to Mn(II), as confirmed by voltammetric and spectroscopic measurements. To confirm that only dissolved Mn(III) was measured, we added a colloidal form of soluble manganese dioxide (*24*) to Black Sea (and Chesapeake Bay) waters and then added DEF-B to the sample. No Mn(III)DEF-B production was observed during the 4-hour measurement period.

Measurements of dissolved Mn(III) were made during a month-long Black Sea research cruise on the *R/V Knorr* in 2003. The cruise had three legs; leg 172-07 (15 to 25 April), leg 172-08 (25 April to May 10), and leg 172-09 (10 to 15 May). Twelve stations in the Black Sea (Fig. 2A) were analyzed for soluble Mn(III) complexes. Several stations were sampled two times on different days, and one station in the central west of the Black Sea was sampled six times over the expedition. The water column of the southwest Black Sea was sampled more intensively because highly saline water enters the Black Sea through the Bosporus Strait and mixes with lower salinity oxygen-rich cold intermediate-layer (CIL) waters. The saline intrusions are pushed eastward by western gyre waters, which have a cyclonic circulation pattern (*20*), and disrupt the thickness of the suboxic zone (defined as $O_2 < 3$ μM and $H_2S < 0.2$ μM).

In each Black Sea depth profile (Fig. 2, B to F; fig. S2), O_2 concentration decreased with depth and density, as a result of organic matter decomposition with O_2 as electron acceptor, to the suboxic zone containing no detectable O_2 and ΣH_2S. ΣH_2S concentrations increased below that zone. The suboxic zone in the eastern and central Black Sea had a thickness of at least 0.50 potential density (σ_t) units (Fig. 2F) (σ_t = 15.61 to 16.13). However, the thickness decreased on proximity to the Bosporus because the west central Black Sea (Fig. 2B, site 9) is ≤ 0.44 σ_t units (15.58 to 16.02) and southwest stations are thinner (e.g., Fig. 2E, site 4, σ_t = 15.80 to 16.15).

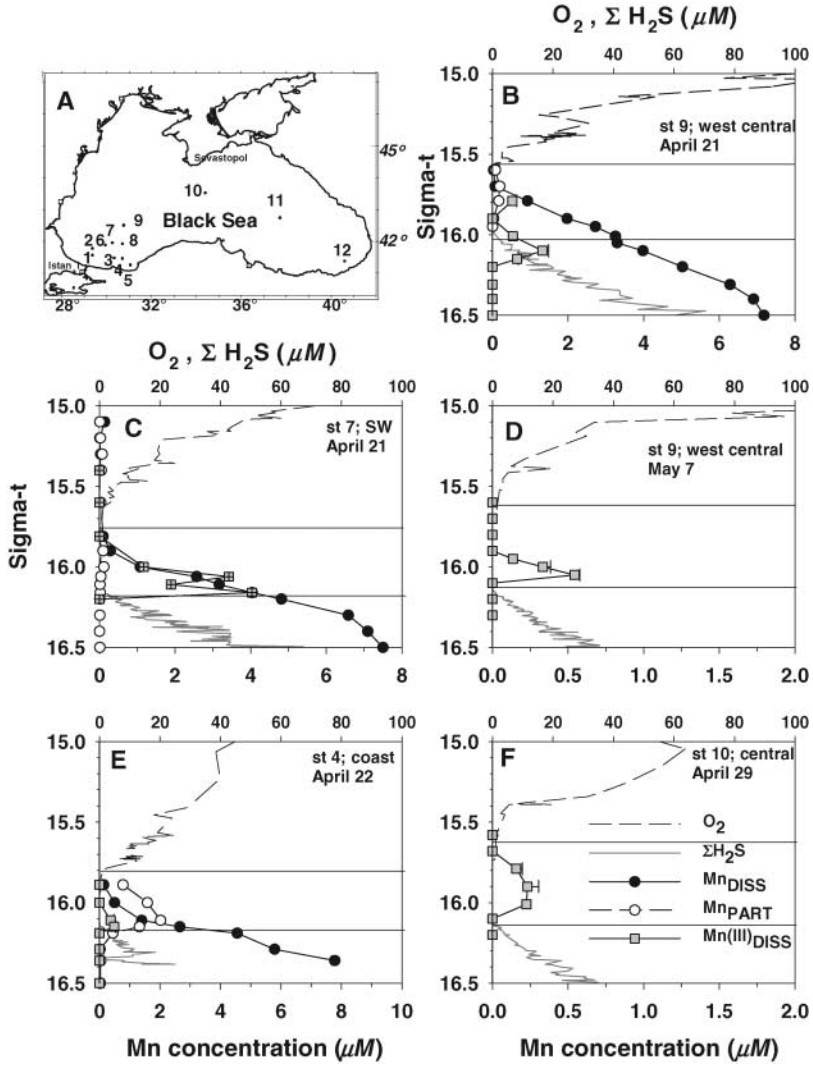

Fig. 2. Map of the Black Sea (**A**), and representative profiles of ΣH_2S, O_2, Mn(III) organic complexes, $Mn_{dissolved}$, and $Mn_{particulate}$ at different stations in the west central (**B** and **D**), southwest (**C** and **E**), and central Black Sea (**F**). ΣH_2S is the sum of H_2S/HS^-, S(0) as S_8, and S_x^{2-}. Particulate and total dissolved manganese measurements for a revisit to site 9 and site 10 (D and F) were not plotted, because those measurements were conducted on a different cast from the dissolved Mn(III) measurements. To compare results at different stations, we plotted chemical species versus potential density (σ_t), and not depth, because the appearance or disappearance of chemical species in the Black Sea follows characteristic density surfaces (*29*). For example, O_2 is last detected at an average σ_t of 15.60, and H_2S is first detected at an average σ_t of 16.15. But O_2 was detected deeper (down to 15.95) in the southwest, where oxygen-rich water intrudes and is pushed eastward by the cyclonic circulation. The suboxic zone thickness ranges from 20 to 40 m. The area between the horizontal lines in (B) to (F) indicates the extent of the suboxic zone for each profile.

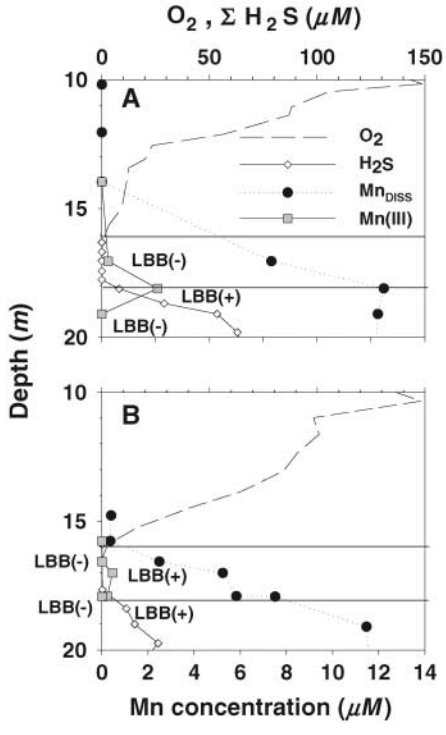

Fig. 3. Two profiles of in situ O_2 and ΣH_2S sampled on the downcast, plotted with total dissolved manganese and dissolved Mn(III) complexes on water sampled from the upcast. Tidal influences can affect the thickness of the suboxic zone within a complete cast. For these casts, the in situ analyzer and the bottles were on the same CTD rosette system. On the upcast, bottle samples and the in situ analyzer did not have a ΣH_2S signal when soluble Mn(III) was detected. (**A**) Cast taken on 3 August 2003 at 19:38 and (**B**) 4 August 2003 at 14:02 and 17:14. LBB(+) and LLB(−) indicate a positive and negative result for leucoberbelin blue (LBB), respectively. The area between the horizontal lines indicates the extent of the suboxic zone for each profile.

Particulate manganese concentrations were typically low (<0.2 μM), except near the coastal zone (Fig. 2E, site 4) where maximum concentrations were 2 μM. Coexistence of oxidized particulate and dissolved manganese and H_2S was not observed in samples from bottles. The apparent overlap of oxidized Mn with the in situ sulfide signal (Fig. 2B) is due to soluble S(0) (*19*) and because the samples came from different casts [additionally, the conductivity-temperature-depth (CTD) sensor and the bottles are offset by 0.5 m; for the cast in Fig. 2B, the σ_t range of 16.00 to 16.15 had a vertical-depth resolution of 6 m versus 13 m for that in Fig. 2D]. Dissolved manganese was present in all samples of the Black Sea's suboxic region, with a maximum concentration of ~8 μM below the H_2S onset (Fig. 2, C and E). Mn(III) complexes were detected at 10 of the 12 investigated stations with the exception of station 2 in the southwest and station 12 in the eastern basin. The highest Mn(III) complex concentrations were measured at stations 6 (5 μM; figs. S2 and S3) and 7 (4 μM; Fig. 2C), where Mn(III) constituted up to 100% of the dissolved Mn at the maximum dissolved Mn concentrations. We conclude that, at these southwestern sites, intrusions of oxygen-rich water from the Bosporus intensified the manganese redox cycle and caused higher production of dissolved Mn(III). In contrast, the central and eastern Black Sea had lower dissolved Mn(III) concentrations, typically just above the detection limit of the analytical method of ~150 nM (Fig. 2F and figs. S2 and S3). For all other suboxic areas, Mn(III) complexes when detected constituted 16 to 56% of the dissolved Mn.

We observed two types of dissolved Mn(III) profiles in the suboxic zone. The more common one (16 of 18 profiles) was a single maximum at the top (Fig. 2, C and D), at the bottom (Fig. 2E), or in the middle (Fig. 2F, fig. S2). The latter was observed at the central and eastern stations 10 and 11, which do not experience lateral O_2 intrusions. The least common profile (2 of 18; e.g., Fig. 2B) showed two distinct maxima at the top and bottom of the suboxic zone and was observed at coastal station 5 (fig. S2C) and west central station 9 (Fig. 2B). The maximum at the top of the suboxic zone (Fig. 2, B to D) occurred just below where O_2 disappeared and as particulate and dissolved manganese started to increase with depth. This maximum is characterized by the one-electron oxidation of Mn(II). Dissolved Mn(III), trapped with chelating agents, is formed during the oxidation of Mn(II) (*16*). Organic matter decomposition with release of photocenter PSII products could also lead to soluble Mn(III). The second maximum occurred at the bottom of the suboxic zone (Fig. 2, B and E), where particulate manganese decreased and the first sulfur species were detected. At this deeper maximum, H_2S reduced MnO_2-forming polysulfides and elemental sulfur [particulate S_8 is 2 μM as S^0; e.g., (*20*)]. The profiles indicate that Mn(III) complexes are formed during the one-electron reduction of MnO_2.

Dissolved Mn(III) profiles (Fig. 2, B and D) measured on the same day (21 April) at the west central site (station 9) were reproducible (not shown), but these profiles were different from the profile measured on 7 May, both in the number of maxima, as well as in maximum Mn(III) complex concentration, 1.4 μM versus 0.6 μM. Winter conditions in March resulted in surface ventilation of the Black Sea's CIL waters (*26*) and persisted past mid-April. The two Mn(III) maxima in April indicate that both Mn(II) oxidation and Mn(IV) reduction occurred and resulted in an active Mn redox cycle. On 7 May, calmer seas reestablished a stable suboxic zone with a less active Mn redox cycle.

We sampled the Chesapeake Bay water column in July 2002, August 2003, and 2004 below the Bay Bridge (8°58.10′ N; 76°21.43′ W). In July 2002, the suboxic region was poorly developed, because a recent storm had mixed the water column. Dissolved Mn(III) complexes were not observed. In contrast, the suboxic zone in 2003 was well developed and had a maximum thickness of 3 m on 3 to 5 August (Fig. 3). We measured six water-column profiles on 3 days (3, 4, and 5 August), and the results confirmed that Mn(III) complexes were present in the suboxic zone of the Chesapeake Bay then. Leucoberbelin blue (LBB) was used to confirm the presence of Mn(III,IV) species and functioned as a secondary indicator for the presence of dissolved Mn(III) complexes in filtered waters (*27*, *28*). The suboxic zone was not stable with depth but moved up and down in the water column with the tidal cycle, as sulfidic bottom waters and oxygenated surface waters were mixed into the suboxic zone.

Typically, filtration has been used to separate the oxidized and the reduced manganese fractions. This method does not discriminate between the presence of soluble Mn(III) complexes and Mn(II), because the formaldoxime reagent reduces oxidized Mn phases that pass through the filter. Earlier studies (*3–5*, *21*, *29*) thus underestimated the oxidizing-reducing capacity of the soluble Mn pool. Also, studies based on these analytical techniques, as well as atomic absorption spectroscopy, underestimated the capacity for microorganisms to affect biogeochemical processes because Mn(III) can be used as either an electron acceptor or donor.

Our data demonstrate that one-electron transfer reactions are more important for Mn biogeochemistry than previously thought. Thus, dissolved Mn(III) will likely be important in other suboxic systems such as plumes from hydrothermal vents and productive rivers, stratified lakes, sedimentary porewaters, and major oxygen minimum zones such as the Arabian Sea and the equatorial Pacific. Depending on the thermodynamic and kinetic stability of the ligands binding Mn(III), Mn(III) should exist at (sub)nanomolar concentrations in oxic waters of lakes and oceans, as has been found for Fe(III) (*30–32*). Mn(III) will also compete with Fe(III) for these ligands (*12*).

References and Notes

1. P. N. Froelich *et al.*, *Geochim. Cosmochim. Acta* **43**, 1075 (1979).
2. G. W. Luther III *et al.*, *Geochim. Cosmochim. Acta* **61**, 4043 (1997).
3. B. M. Tebo, *Deep-Sea Res.* **38** (Suppl. 2A), S883 (1991).
4. B. M. Tebo, R. A. Rosson, K. H. Nealson, in *Black Sea Oceanography*, E. Izdar, J. W. Murray (Eds.) (Kluwer, Dordrecht, the Netherlands, 1991), pp. 173-185.
5. D. J. Burdige, K. H. Nealson, *Geomicrobiol. J.* **4**, 361 (1986).
6. G. W. Luther III, T. M. Church, D. Powell, *Deep-Sea Res.* **38** (Suppl. 2A), S1121 (1991).
7. F. J. Millero, *Deep-Sea Res.* **38** (Suppl. 2A), S1139 (1991).
8. W. Yao, F. J. Millero, *Geochim. Cosmochim. Acta* **57**, 3359 (1993).
9. K. M. Faulkner, R. D. Stevens, I. Fridovich, *Arch. Biochem. Biophys.* **310**, 341 (1994).
10. J. K. Klewicki, J. J. Morgan, *Environ. Sci. Technol.* **32**, 2916 (1998).
11. J. E. Kostka, G. W. Luther III, K. H. Nealson, *Geochim. Cosmochim. Acta* **59**, 85 (1995).
12. D. L. Parker, G. Sposito, B. M. Tebo, *Geochim. Cosmochim. Acta* **68**, 4809 (2004).
13. J. S. Summers *et al.*, *Inorg. Chem.* **44**, 3405 (2005).
14. O. W. Duckworth, G. Sposito, *Environ. Sci. Technol.* **39**, 6037 (2005).
15. G. W. Luther III, *Geomicrobiol. J.* **2**, 195 (2005).
16. S. M. Webb, J. R. Bargar, B. M. Tebo, *Proc. Natl. Acad. Sci. U.S.A.* **102**, 5558 (2005).
17. P. S. Nico, R. J. Zasoski, *Environ. Sci. Technol.* **35**, 3338 (2001).
18. P. J. Brendel, G. W. Luther III, *Environ. Sci. Technol.* **29**, 751 (1995).
19. T. F. Rozan, S. M. Theberge, G. W. Luther III, *Anal. Chim. Acta* **415**, 175 (2000).
20. S. K. Konovalov *et al.*, *Limnol. Oceanogr.* **48**, 2369 (2003).
21. P. G. Brewer, D. W. Spencer, *Limnol. Oceanogr.* **16**, 107 (1971).
22. W. G. Sunda, S. Huntsman, *Limnol. Oceanogr.* **32**, 552 (1987).
23. W. G. Sunda, S. Huntsman, *Limnol. Oceanogr.* **35**, 325 (1990).
24. J. F. Perez-Benito, E. Brillas, R. Pouplana, *Inorg. Chem.* **28**, 390 (1989).
25. B. M. Tebo *et al.*, *Annu. Rev. Earth Planet. Sci.* **32**, 287 (2004).
26. M. C. Gregg, E. Yakushev, *Geophys. Res. Lett.* **32**, 1 (2005).
27. W. Krumbein, H. J. Altmann, *Helgol. Wiss. Meeresunters.* **25**, 347 (1973).
28. K. H. Nealson, B. M. Tebo, R. A. Rosson, *Adv. Appl. Microbiol.* **33**, 279 (1988).
29. J. W. Murray *et al.*, in *Aquatic Chemistry: Interfacial and Interspecies Processes*, C. P. Huang, C. R. O'Melia, J. J. Morgan, Eds. (American Chemical Society, Washington, DC, 1995), vol. 244, pp. 157–176.
30. M. Gledhill, C. M. G. van den Berg, *Mar. Chem.* **47**, 41 (1994).
31. E. L. Rue, K. W. Bruland, *Mar. Chem.* **50**, 117 (1995).
32. J. Wu, G. W. Luther III, *Mar. Chem.* **50**, 159 (1995).

33. We thank the crew and Captain A. D. Colburn of the *R/V Knorr* for their help. We thank G. Druschel, C. Kraiya, G. Dick, C. Sheehan, K. Murray, and R. Howard for aid in sampling and analyses. B.G.C. was supported in part by a National Defense Science and Engineering Graduate fellowship. This work was funded by grants from the NSF to G.W.L. (OCE-0096365) and B.M.T. (OCE-0221500).

Supporting Online Material

www.sciencemag.org/cgi/content/full/313/5795/1955/DC1
Materials and Methods
Figs. S1 to S3
References

21 July 2006; accepted 15 August 2006;
10.1126/science.1132876